JOURNAL OF VIROLOGY, Oct. 1996, p. 6909–6921 Vol. 70, No. 10
0022-538X/96/$04.00+0

A Vaccinia Virus Core Protein, p39, Is Membrane Associated

SALLY CUDMORE,[1] RAFAEL BLASCO,[2] RENAUD VINCENTELLI,[3] MARIANO ESTEBAN,[4] BEATE SODEIK,[1]† GARETH GRIFFITHS,[1]* AND JACOMINE KRIJNSE LOCKER[1]

Cell Biology Program[1] and Structures and Biocomputing Program,[3] European Molecular Biology Laboratory, D-69117 Heidelberg, Germany, and Centro de Investigación en Sanidad Animal, INIA-MAPA, Valdeolmos, 28130 Madrid,[2] and Centro Nacional de Biotecnología, Consejo Superior de Investigaciones Científicas, Campus Universidad Autónoma, 28049 Madrid,[4] Spain

Received 11 March 1996/Accepted 5 July 1996

We describe herein the characterization of p39, the product of the A4L gene of vaccinia virus. By immunolabelling of thawed cryosections from infected HeLa cells, we show that this protein is initially located in the central region, or viroplasm, of the viral factories, as well as in the immature virions, with very small amounts of labelling observed on the surrounding membranes. The localization of p39 changes dramatically during the transition of the immature virion to the intracellular mature virus (IMV), coincident with the appearance of the core structure in the center of the IMV, with p39 located between this core and the surrounding membranes. Complementary biochemical data, such as partitioning into the Triton X-114 detergent phase and stripping of the viral membranes with Nonidet P-40 and dithiothreitol, suggest that p39 is associated with the innermost of the two membranes surrounding the core. Sodium carbonate treatment also indicates that p39 is associated with membranes, even at the early stages of viral assembly. However, following in vitro translation of p39 in the presence of microsomal membranes, we failed to detect any association of the independently expressed protein with membranes. We also failed to detect any posttranslational acylation of p39 with myristate or palmitate, suggesting that p39 does not achieve its membrane association through lipid anchors. Therefore, p39 is most likely membrane associated through an interaction with an integral membrane protein(s) present in the innermost of the two membranes surrounding the IMV. These data, together with our recent data showing that p39 colocalizes with the spike-like protrusions on the IMV core (N. Roos, M. Cyrklaff, S. Cudmore, R. Blasco, J. Krijnse-Locker, and G. Griffiths, EMBO J. 15:2343–2355, 1996), suggest that p39 may form part of this spike and that it possibly functions as a matrix-like linker protein between the core and the innermost of the two membranes surrounding the IMV.

Vaccinia virus, the prototype member of the *Poxviridae*, has a 190-kb double-stranded DNA genome, which has been completely sequenced (18, 26). This genome codes for 263 potential open reading frames, the products of which include approximately 100 proteins that are associated with the virus particle (13). The transcription and translation of these genes can be divided into three temporal classes: early, intermediate, and late (38, 43). The early genes are those which are transcribed prior to DNA replication, while the intermediate and late genes are only transcribed during or after replication of the viral genome. The vaccinia virus structural proteins are normally encoded by the late genes (38).

Vaccinia virus assembly has been extensively studied by electron microscopy (EM), but little is known about the molecular events which take place during the assembly process. The first morphological evidence of the infection process is the appearance of large structures enriched in DNA (2, 21, 27) at about 1 to 2 h postinfection (p.i.). These structures, which are also visible by light microscopy, are referred to as viral factories and are thought to be the site of viral DNA replication and transcription (2, 38, 39). The first sign of viral membrane assembly is the appearance of rigid, curved membrane structures referred to as crescents, which appear to bud in the region of the viral factories. Originally thought to be the only example of de novo membrane synthesis (6, 7, 60), more recent evidence suggests that these first membranes of vaccinia virus are derived from a cisterna of the intermediate compartment between the rough endoplasmic reticulum and the Golgi complex (31, 54). Although by EM these crescents, which are the progenitors of the immature virion (IV), appear as a single membrane profile, our recent data strongly suggested that they consist of two tightly apposed membrane bilayers (54). The spherically shaped IV develops a core structure surrounding the DNA and matures into the brick-shaped intracellular mature virus (IMV), the first of two distinct infectious forms. This process coincides with the cleavage of some of the core proteins (28, 29, 41, 50, 57, 58).

There is a marked difference in structure between the IV and the IMV. The IMV has two membrane-like profiles when viewed by both conventional thin sectioning and cryo-EM, the innermost of them representing the newly formed core structure. We believe that the outer profile is qualitatively the same as the two membranes surrounding the IV; i.e., it may represent the two tightly apposed membranes derived from the intermediate compartment (48, 54). While the central region of the IV clearly consists of electron-dense material that can be labelled with antibodies to vaccinia virus core proteins (12, 55, 59), it does not yet contain the final internal core structure (see, e.g., reference 12). Nothing is known about either the origin or the composition of this inner membrane-like core structure or about how it is formed during the transition from IV to IMV. A possible explanation for the appearance of the core during the assembly process may be that the insertion of the DNA into the IV (see reference 37), which coincides with the proteolytic cleavage of some of the major core proteins (28, 29, 41, 57, 58, 61), leads to a rearrangement of these core proteins to form the core structure. Following this process, the

* Corresponding author. Mailing address: Cell Biology Program, European Molecular Biology Laboratory, Meyerhofstrasse 1, D-69117 Heidelberg, Germany. Phone: (49) (6221) 387267. Fax: (49) (6221) 387306.

† Present address: Department of Cell Biology, Yale University School of Medicine, New Haven, CT 06520-8002.

IMV membranes appear brick shaped rather than spherical, as they were in the IV. This change in shape may result from an interaction of one or several inner membrane proteins with components on the surface of the newly formed core.

In pioneering EM studies of IMV particles, using a combination of thin sectioning and negative staining, Dales (5) clearly showed the presence of spike-like protrusions extending between the core and the surrounding membranes. In a more recent study, Dubochet et al. (10) performed cryo-EM, a method that does not involve chemical fixation, dehydration, or embedding techniques, on intact IMV as well as on isolated vaccinia virus cores. These isolated cores are operationally defined as the particles which remain intact after treatment of IMV with Nonidet P-40 (NP-40) and a reducing agent, such as dithiothreitol (DTT) or β-mercaptoethanol (11, 45, 56). In the later studies, the spikes were clearly visualized on the outer surface of the isolated cores, as well as in untreated IMV. These data were extended by combining cryo-EM with immunogold labelling of antigens on the surface of the core (48), which suggested that these spike-like protrusions may be composed of p39, the focus of this paper.

p39 was first identified by Maa and Esteban (35) as a highly antigenic protein that elicited a strong immune response in mice and rabbits. They demonstrated that p39, a product of the late class of genes, is an acidic polypeptide which is present in the vaccinia virus core. The protein was later identified as the product of the A4L gene, and it was established that the C-terminal 103 amino acids were the most immunogenic region of the protein, eliciting an antibody response in vaccinated humans which persists for years (8). Because of both its location on the outside of the core and its abundance in virions, we suspected that p39 might play an important role during the transition of the IV to the IMV. We therefore attempted to establish a function for p39 during virion assembly and maturation. We propose that p39 plays a matrix-like role in the virion, acting as a link between the core and the surrounding membranes in the IMV.

MATERIALS AND METHODS

Cells, virus, and antibodies. HeLa cells were grown and infected with vaccinia virus WR as previously described (54). Two different antibodies were used in the present study. First, we used the rabbit antiserum raised against p39 previously described by Demkowicz et al. (8). In addition, we made a new rabbit polyclonal antibody. A peptide representing C-terminal residues 267 to 281 of the protein product of gene A4L (pI, 10.78) was solubilized in phosphate-buffered saline (PBS) prior to being covalently coupled to keyhole limpet hemocyanin. Rabbits were immunized with 200 μg of peptide in Freund's complete adjuvant (Sigma) in the popliteal lymph node on day 1. They received subscapular boosts of 50 μg of peptide in Freund's incomplete adjuvant (Sigma) on days 21 and 42, and 50 ml of blood was taken from each animal 10 days after each boost. On day 63, each rabbit received an intramuscular boost of 25 μg of peptide in PBS, and this was followed by intravenous boosts of 25 μg on 2 consecutive days. Ten days later, the animals were sacrificed and sera were prepared. Western blot (immunoblot) analysis showed that this peptide antibody recognized p39. This peptide antibody was used for the immunofluorescence studies, while the other p39 antiserum (8) was used in all other experiments.

Metabolic labelling of virus and infected cells. Four 175-cm^2 flasks of subconfluent HeLa cells were infected at a multiplicity of infection of 10. Two millicuries of ^{35}SExpress (Du Pont, New England Nuclear Research Products, Boston, Mass.) in 20 ml of labelling medium (10% minimal essential medium [MEM] containing 5% fetal calf serum [FCS], 90% methionine- and cysteine-free Dulbecco's MEM [Sigma]) was added to the infected cells at 6 h p.i. After 24 h of infection, the radioactive label was chased for 2 h by replacing the labelling medium with MEM containing 5% FCS. The virus was purified by centrifugation (SW40 rotor, 24,000 rpm) through sedimentation in a 36% sucrose cushion followed by a 15 to 40% sucrose gradient (9). ^{35}S-labelled postnuclear supernatant (PNS) from infected cells was prepared as follows. HeLa cells were infected as described above and incubated in MEM-FCS containing 100 μg of rifampin (Sigma) per ml. The cells were labelled with 40 μCi of ^{35}SExpress in labelling medium from 6 to 8 h p.i. and chased for 1 h, still in the presence of rifampin. Cells were then scraped from the dish in calcium-free PBS, gently pelleted, and resuspended in 10 mM Tris-Cl, pH 9. The cells were broken by 10 to 12 strokes of a Dounce homogenizer, and the nuclei were removed by centrifugation in an Eppendorf centrifuge (Biofuge; Heraeus Christ) at 3,000 rpm for 10 min. For the pulse-chase analysis, infected cells were pulse-labelled for 5 min with 100 μCi of ^{35}SExpress per ml at 7 h p.i. and subsequently chased for various periods of time. The labelled cells were lysed as described previously (30), the lysates were concentrated by acetone precipitation at −20°C, and the precipitate was dissolved in first-dimension lysis buffer (9.8 M urea; 2% ampholines [Pharmacia, Uppsala, Sweden], pH 7 to 9; 4% NP-40; and 100 mM DTT).

For preparation of PNS labelled with either [^{3}H]myristate or [^{3}H]palmitate (250 μCi of each per ml) (14), the labelled lipids were added to infected cells, in Dulbecco's MEM with 2% delipidated FCS (3), 4 h after infection. PNS was prepared at 24 h p.i., as described above. For preparation of ^{32}P-labelled PNS, infected cells were starved of phosphate for 30 min (in Dulbecco's MEM without Na_2PO_4 but containing 2% dialysed FCS) prior to addition of 400 μCi of ^{32}P at 6 h p.i. The labelled cells were harvested at 24 h p.i., and a PNS was prepared as described above. [^{3}H]glucosamine labelling was carried out in RPMI medium (glucose free) containing 2% dialyzed FCS, 2 mM glutamine, and 10 μg of glucose per ml. [^{3}H]glucosamine (75 mCi/ml) was added to a 3-cm-diameter dish of cells at 4 h p.i., and PNS was prepared at 24 h p.i. Immunoprecipitation with antibodies to p39 (8) or p21 (A17L) (31) was carried out as previously described (30), followed by sodium dodecyl sulfate-polyacrylamide gel electrophoresis (SDS-PAGE) analysis (15% polyacrylamide gels).

Protein microsequencing. Purified IMV was resolved by SDS–15% PAGE. After electrophoresis, the gel was stained with Coomassie brilliant blue (R250), and a band that comigrated with p39 on Western blots was excised. The gel piece was subjected to tryptic digestion, the peptides were separated by high-performance liquid chromatography, and two resulting peptides were sequenced by Edman automated degradation (32). The two 7-amino-acid sequences were used to search Swissprot data bank (using Blitz), the Brookhaven data bank, PIR, and Swissprot (using Blast), and GenBank and the EMBL Data Library (using TFasta) for sequences exhibiting homology. These peptides are identical to amino acids 42 to 50 and 59 to 66 of the vaccinia virus WR strain A4L gene (AC P29191).

Immunofluorescence microscopy. Cells grown on coverslips were infected as described above and, following three washes in PBS, were fixed at 8 h p.i. with 3% paraformaldehyde in CB (10 mM MES [morpholineethanesulfonic acid], 150 mM NaCl, 5 mM EGTA, 5 mM $MgCl_2$, 5 mM glucose; pH 6.1) for 10 min at room temperature. Following three washes in CB, cells were permeabilized with 0.1% Triton X-100 (TX-100) for 60 s and then blocked with 1% FCS and 1% bovine serum albumin (BSA) for 10 min. The infected cells were labelled with the antiserum against the C terminus of p39 (diluted 1:300) for 30 min and subsequently incubated with fluorescein isothiocyanate-conjugated goat anti-rabbit antibody (Dianova-immunotech GmbH, Hamburg, Germany) together with 5 μg of Hoechst strain (no. 33258; Sigma) per ml for 30 min. The coverslips were washed three times in CB, rinsed in distilled water, and mounted on slides in Moviol. The samples were examined with a Zeiss Axiophot microscope.

EM. For negatively stained samples, IMV was adsorbed to a glow-discharged, Formvar- and carbon-coated EM grid for 2 min. The sample on the grid was subsequently treated with either 1% NP-40 or 20 mM DTT, or both, for 30 min at 37°C. The IMV which had adsorbed to the grid was also treated with either 50 μg of proteinase K per ml for 30 min on ice or 50 μg of trypsin per ml for 30 min at 37°C. Following three washes in 10 mM Tris (pH 9), the grids were incubated first with 10% FCS in PBS and subsequently with primary antibody (p39 antiserum [8] or a monoclonal antibody against p14, C3 [46]), diluted in 5% FCS–PBS for 15 min. In the case of p14, the labelling was followed by incubation with a rabbit anti-mouse antibody (Cappel, Durham, N.C.). Subsequently, the grids were incubated for 15 min with 10-nm protein A-gold and then briefly washed in triple-distilled water before being stained with 1.5% uranyl acetate for 60 s (53).

Cells which were infected for 8 h, and cells which were infected in the presence of rifampin for 16 h, were fixed and prepared for cryosectioning and immunolabelling with anti-p39 (8) as previously described (19, 55).

Purified IMV was prepared for EM by pelleting for 10 min at 14,000 rpm in an Eppendorf centrifuge and were then fixed with 4% paraformaldehyde–0.1% glutaraldehyde for 30 min. The pellet was subsequently infiltrated with 2.1 M sucrose for 15 min and then rapidly frozen in liquid nitrogen. Immunolabelling of frozen hydrated cryosections was performed as previously described (49, 53, 54).

Protease treatment. Purified IMV was incubated on ice for 30 min with proteinase K (Merck, Darmstadt, Germany) at 5, 10, 20, 30, 50, 100, 200, and 300 μg/ml in 10 mM Tris, pH 9.0 (made from a 1-mg/ml stock solution in isopropanol which was stored at −80°C). Reactions were stopped by the addition of phenylmethylsulfonyl fluoride (Sigma) (10 mM stock solution, in isopropanol, stored at −20°C) to a final concentration of 1 mM. Purified virus was also treated with 50 μg of α-chymotrypsin (TLCK treated; Sigma) per ml (stock solution, 1 mg/ml, stored at −20°C), 100 μg of thermolysin (Boehringer GmbH, Mannheim, Germany) per ml (stock solution, 10 mg/ml in 20 mM $CaCl_2$, stored at −20°C), and 250 μg of V8 (endoproteinase Glu-C; Boehringer) per ml (stock solution, 10 mg/ml, stored at −20°C). All incubations were carried out for 30 min at 37°C. The reactions were terminated by the addition of 3,4-dichloroisocoumarin (Boehringer), to a final concentration of 0.1 mM (stock solution, 40 mM, stored at −20°C), to the chymotrypsin- and V8-treated samples and 5 mM EDTA (Merck) to the thermolysin sample. The samples were immediately frozen in liquid nitrogen and stored at −20°C to prevent further digestion. All samples

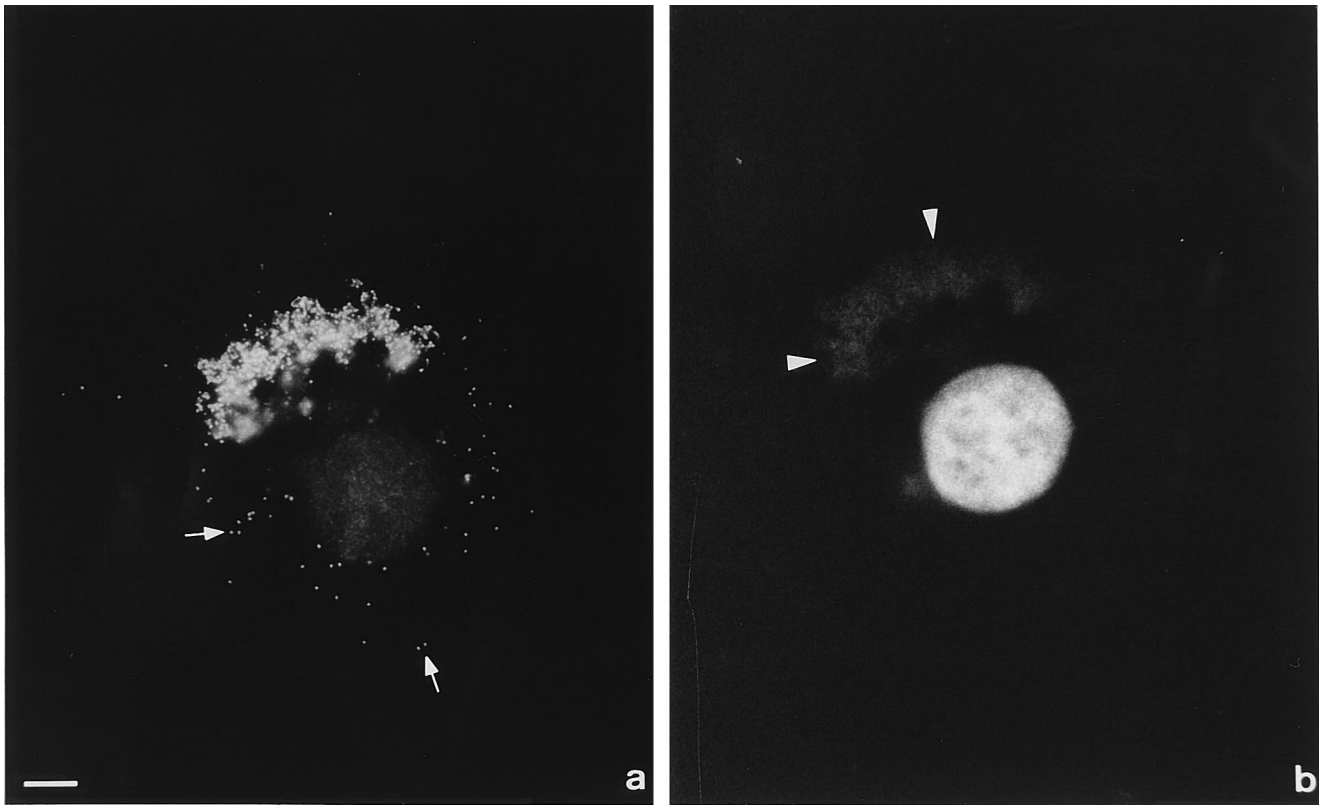

FIG. 1. Immunofluorescence localization of p39 in vaccinia virus-infected HeLa cells 8 h after infection. (a) An infected cell labelled with antibodies against the C terminus of p39. There is strong labelling of the perinuclear region of the cell, most likely corresponding to the viral factories. (b) DNA visualized by Hoechst stain. Arrowheads indicate viral factories. The punctate structures seen throughout the cell (arrows) probably represent individual virions. Bar, 20 μm.

were heated for 3 min at 95°C in Laemmli sample buffer just prior to electrophoresis.

Detergent extraction and sodium carbonate treatment of IMV and PNS. Viral membranes were separated from the cores as described by Oie and Ichihashi (45) with the following modifications: virus was (i) disaggregated before treatment by a 30-s sonication in a water bath sonicator and (ii) incubated with 1% NP-40 (Sigma) and 20 mM DTT (Sigma) in 10 mM Tris (pH 9) rather than 100 mM Tris (pH 7.5). The incubation was carried out for 30 min at 37°C with gentle shaking. The sample was then loaded on top of a 36% sucrose cushion and spun in an Airfuge at 26 lb/in^2 for 30 min to separate the membranes, which remained on top of the sucrose cushion, from the cores, which pelleted. The cores were subsequently incubated with 0.5% deoxycholate (Sigma) and 0.5% SDS (Serva) at 56°C for 10 min to ensure solubilization prior to adding Laemmli sample buffer.

For the TX-114 extraction (1), following a brief sonication, intact virus was solubilized in an equal volume of 2% TX-114–300 mM NaCl–1 mM DTT–10 mM Tris (pH 10). An additional 400 μl of 1% TX-114–150 mM NaCl–10 mM Tris (pH 9) was added, and the mixture was incubated at 37°C for 15 min followed by 20 min at 4°C and a 2-min centrifugation at 14,000 rpm in an Eppendorf centrifuge to separate the phases. Both phases were subjected to a second round of TX-114 extraction. TX-114 extraction of radiolabelled PNS from cells infected in the presence of rifampin (see above) was performed in the same way, except that the DTT was omitted. For the Na_2CO_3 extraction of PNS from cells infected in the presence of rifampin, the pH of the sample was adjusted to 11 by the addition of an equal volume of 200 mM Na_2CO_3. The sample was incubated for 30 min on ice and then spun at 150,000 × *g* (Beckman TLA100 rotor) to pellet the membranes. All samples were concentrated by acetone precipitation at −20°C, and the pellets were dissolved in Laemmli sample buffer or first-dimension lysis buffer prior to electrophoresis.

Cloning, transfection, and in vitro translation of A4L. Gene A4L from vaccinia virus strain WR was PCR amplified with the following primers: TCGGAATTCAATTTTAAAGC (*Eco*RI site underlined) and TTTACTCGAAAAGCTTGATT (*Hin*dIII site underlined). It was then digested with *Eco*RI and *Hin*dIII and inserted into plasmid pGEM7. p39 was transcribed and translated in vitro by using pGEMA4L and a coupled T7-driven transcription-translation system (Promega) in accordance with the instructions of the manufacturer. When dog pancreas microsomes (a kind gift from K. Schroeder and B. Dobberstein) were used, they were added at 100 optical density units (optical density at 280 nm) per translation. To remove endogenous mRNA, the microsomes were treated with micrococcal nuclease (Sigma) before translation (31). Soluble p39 was separated from (putative) membrane-bound protein by pelleting the membranes in a Beckman Airfuge through a cushion of 0.5 M sucrose in RM buffer (50 mM HEPES [*N*-2-hydroxyethylpiperazine-*N*′-2-ethanesulfonic acid]-KOH, pH 7.5; 50 mM potassium acetate; 2 mM magnesium acetate; 1 mM DTT) for 10 min at 24 lb/in^2. All fractions were diluted in 500 μl of detergent solution, and SDS was added to a final concentration of 0.2% along with 2 μl of the anti-p39 antibody (8). The subsequent immunoprecipitation steps (as described in reference 31) were followed by analysis by SDS-PAGE.

Gel electrophoresis and Western blotting. Proteins were separated by standard SDS-PAGE (34) with a 15% resolution gel and a 4% stacking gel. Samples were incubated in Laemmli sample buffer containing 1% SDS and 0.5% β-mercaptoethanol for 5 min at 95°C. In some experiments, samples dissolved in first-dimension lysis buffer were subjected to two-dimensional (2D) gel analysis with a Bio-Rad (Richmond, Calif.) mini-two-dimensional gel system. Samples were separated by isoelectric focusing from pH 4.0 to 7.0 in the first dimension and SDS–15% PAGE in the second dimension. The gels were either fluorographed with Entensify (du Pont de Nemours, Brussels, Belgium) or electrophoretically transferred to nitrocellulose membranes for immunoblotting by use of the Bio-Rad semidry transfer system. The nitrocellulose was blocked in PBS with 0.2% Tween 20 and 5% nonfat skim milk (PBS-T milk) overnight at 4°C prior to incubation with anti-p39 serum (8) diluted 1:10,000 in PBS-T milk. The nitrocellulose was then incubated with horseradish peroxidase-tagged goat anti-rabbit antibody (Bio-Rad). Antibody was detected by enhanced chemiluminescence (Amersham Life Sciences, Amersham, England).

Gel filtration. In vitro-translated p39 was resolved by high-performance size exclusion chromatography (Gilson, Villiers-le-Bel, France). The 5-μm TSKG2000 SWXL column (Toyosoda Inc., Tosohaas, Stuttgart, Germany) was precalibrated with a mixture of gel filtration molecular mass standards (ferritin, 440 kDa; catalase, 232 kDa; BSA, 66 kDa; carbonic anhydrase, 29 kDa; and cytochrome *c*, 12.4 kDa). The column was then preequilibrated with 50 mM Na_2PO_4–100 mM KCl, pH 7.4, and 1 μl of sample was injected into the column.

RESULTS

Identification of p39 (A4L) and synthesis of antibodies. As a first step towards the characterization of p39, we decided to ensure its identity by performing peptide sequencing. A 43-

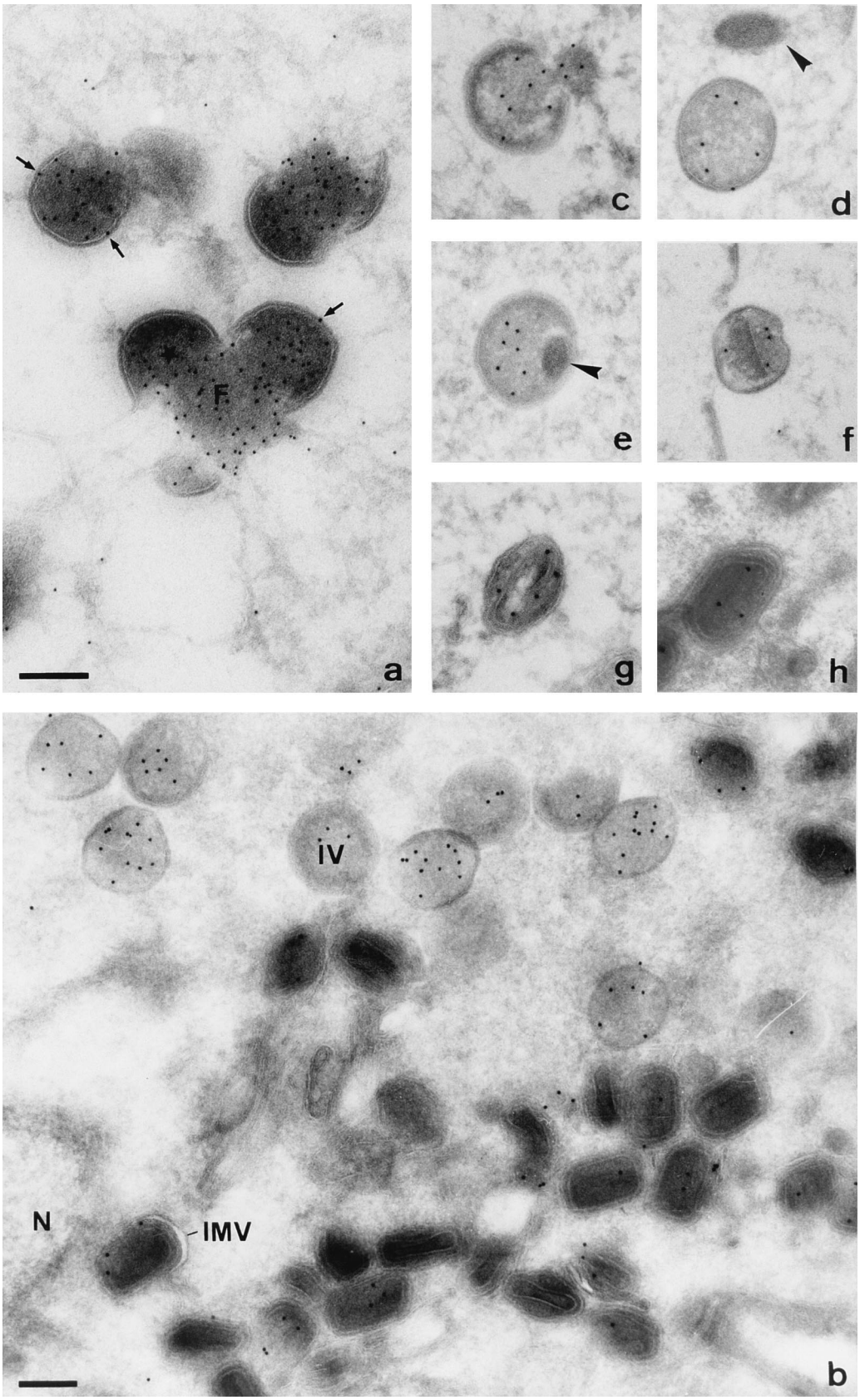
F
a
c
d
e
f
g
h
IV
N
IMV
b

kDa band, reactive by immunoblotting with the antiserum raised against the complete p39 (8), was excised from an SDS-polyacrylamide gel on which purified IMV had been applied and then sequenced by Edman degradation. Two peptides were found that showed 100% homology to the gene product of the vaccinia virus WR A4L open reading frame. This protein has a predicted molecular mass of 30.9 kDa, but since it has previously been referred to as p39 because of its mobility on gels (8, 35), we adhere to this terminology throughout this paper. To facilitate further characterization studies, we raised a COOH-terminal peptide antibody against residues 267 to 281 of p39 which also recognized p39 on Western blots (see Fig. 6a).

p39 labels viral factories, as evidenced by immunofluorescence microscopy. We first investigated the localization of p39 in infected cells by light microscopy. Infected HeLa cells were fixed at 8 h p.i. and labelled with the COOH-terminus-specific peptide antiserum. As can be seen from Fig. 1, clear labelling of structures in the perinuclear region of the cell could be detected. This labelling colocalized with the viral DNA factories, which were visualized by Hoechst staining (Fig. 1b, arrowheads). In addition, p39 antiserum decorated punctate structures throughout the cell, which probably represent individual virus particles (Fig. 1a, arrows).

EM localization of p39. A more precise localization of p39 throughout the different stages of viral assembly was subsequently carried out by immunolabelling thawed cryosections from aldehyde-fixed infected cells. The earliest viral structures to appear in infected cells are termed viral factories (2, 21, 27) (F in Fig. 2a). These electron-dense structures, which are predominantly found in the perinuclear region, are labelled strongly by antibodies against p39 in their central region. From these viral factories, crescent-shaped membranes develop (Fig. 2a). p39 preferentially associated with the viroplasm underlying these membranes, with a very small amount of label occasionally visible on the membranes themselves (Fig. 2a, arrows). These crescents eventually form IVs (Fig. 2b) which are labelled by anti-p39 antibodies throughout the electron-dense viroplasm. The labelling with anti-p39 at these different early stages of assembly resembles the pattern that is seen with antibodies against vaccinia virus core proteins, such as 4a (the processed form of the gene product of A10L, one of the major core proteins) or p65 (D13L) (12, 55, 59).

As the virus particles matured to form IMV (Fig. 2b and g), the p39 labelling was found predominantly in the space between the newly developed core structure and the outer IMV membranes, i.e., in the space between the two visible IMV membrane profiles (see the introduction). Figures 2c to h depict, by p39 labelling, what we believe to be the different stages of vaccinia virus assembly. Figures 2c and d show developing IVs. The viroplasm which is present in these structures is labelled strongly by anti-p39. These IVs are apparently devoid of DNA, which is visible above the virion in Fig. 2d (arrowhead). Figure 2e shows an IV in which an electron-dense structure, most likely the DNA, is visible at one side of the particle (arrowhead). A transitional intermediate between the IV and the IMV is shown in Fig. 2f, where the core structure is beginning to form. At this stage of development, p39 appears to be excluded from the center of the developing core and is found in the space between this structure and the surrounding IMV membranes. The IMV (Fig. 2g) and intracellular enveloped virus (Fig. 2h) also show labelling of the space between the core and the surrounding membranes.

We also investigated the localization of p39 in cells which were infected in the presence of rifampin, which blocks viral assembly prior to the IV stage (20, 40, 44). In these cells, the typical electron-dense structures, previously called rifampin bodies (RB in Fig. 3a) (20, 44, 55), were observed in the cytoplasm close to the nucleus (N in Fig. 3a). Like the viral factories, the rifampin bodies were strongly and uniformly labelled throughout by antibodies against p39. These rifampin bodies were surrounded by membrane structures which, after release of the rifampin block, are thought to form the characteristic crescent-shaped membranes (Fig. 3b, stars). There was only a very small amount of p39 labelling on these membranes (within the ~20-nm resolution of this labelling method [18]), whereas the core material labelled very strongly. As maturation continued, the IVs developed (Fig. 3b), and the viroplasm of the IVs labelled strongly with p39. In addition to the rifampin bodies, another especially distinct structure can be observed in cells infected in the presence of rifampin (11, 52, 53, 54). These accumulations of DNA (D in Fig. 3a and b), which are prevented from being packaged into virions because of the rifampin block, consequently pack into crystalline arrays, which are much larger than those seen in normally infected cells (11, 52, 53, 54). These rifampin-induced periodic DNA structures were also devoid of any p39 labelling.

The localization of p39 in the IMVs was subjected to a closer inspection by processing purified IMV for cryosectioning and subsequent immunolabelling with anti-p39 (Fig. 3c). In these sectioned particles, spike-like protrusions, which have been previously described (5, 10, 48), extend outward from the internal core structure (Fig. 3c, arrowheads). The structure, composition, and function of these spikes are unknown. Recent evidence makes it conceivable that the spikes may be in part composed of p39 (48), and the p39 labelling of the region in Fig. 3c where the spikes are visible further supports this possibility.

Immunolabelling of intact and treated IMV particles. In order to confirm the localization of p39, EM experiments were performed in which purified IMV preparations were subjected to different treatments on the EM grids, followed by immunolabelling and negative staining. Intact IMV particles were not labelled significantly by antibodies against p39 (Fig. 4a). This is in stark contrast to the labelling obtained for another vaccinia virus protein, p14 (A27L) (Fig. 4b), previously described as being exposed on the outside of the virion (53). As can be seen in Table 1, intact IMV became labelled with anti-p39 only occasionally, with an average of less than one gold particle per virion. A small proportion of particles which were disrupted by the preparation also were labelled strongly (data not shown). On treatment of the particles with NP-40 and DTT, classical methods for removing IMV membranes (11, 45), the labelling

FIG. 2. Immunolabelling of thawed cryosections of fixed HeLa cells, infected with vaccinia virus for 8 h, with antibodies against p39. (a) A viral factory (F) labels strongly with anti-p39. Crescent-shaped membranes (star) are visible, protruding from the factories, which display a very small amount of p39 labelling (arrows). (b) The central regions of IVs are clearly labelled by antibodies produced against p39. In the IMV, p39 labelling is observed in the space between the core and the envelope. N, nucleus. (c to h) Virus particles, at various stages during maturation, labelled with anti-p39. (c) A developing IV is packaging viroplasm. (d) The IV is apparently devoid of DNA, which is visible above the particle in a crystalline-like array (arrowhead). (e) An IV is shown that contains an electron-dense structure (arrowhead), most likely representing DNA, which is devoid of p39 labelling. (f) An intermediate stage between the IV and IMV shown in which the label starts to associate with what is interpreted to be the surface of the developing core. (g) The IMV (g) and intracellular enveloped virus (h) are labelled between the core and the IMV membranes. Bars, 200 nm.

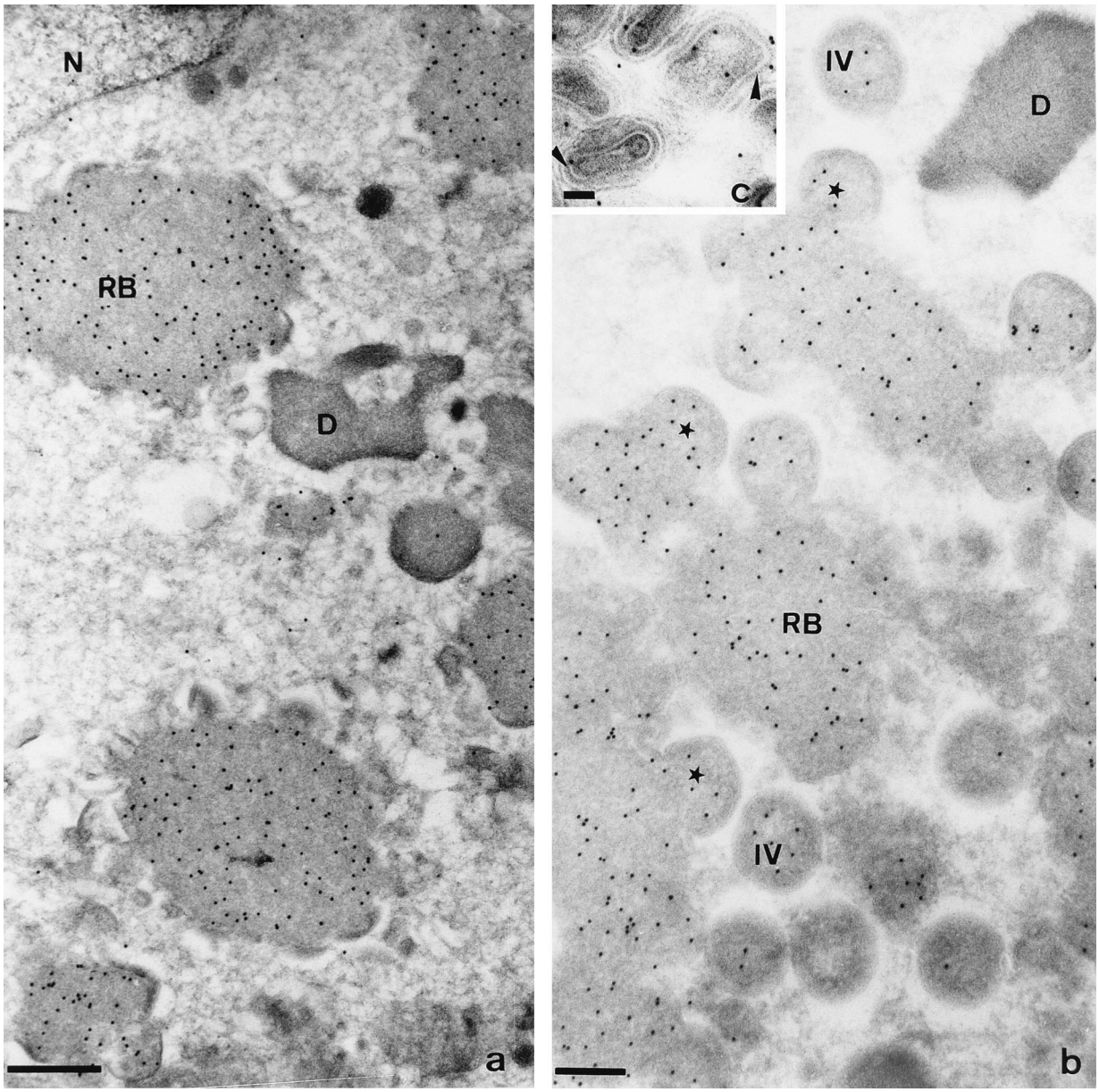

FIG. 3. Cryosections of cells infected for 16 h in the presence of rifampin and immunolabelled with anti-p39. (a) Rifampin bodies (RB), which label strongly with antibodies against p39, are clearly visible. Also visible are crystalline arrays of DNA (D) which are devoid of labelling. N, nucleus. (b) Viral crescents (stars) protruding from the rifampin bodies, as well as IVs, are seen here 15 min after rifampin release. (c) Purified IMVs were used to make pellets, which were cryosectioned and labelled with anti-p39. The label is most frequently found in the region between the core and surrounding IMV membranes, in the same area as the spikes, which extend between the core and IMV membranes (arrowheads). Bars, 400 nm (a), 250 nm (b), and 50 nm (c).

with p39 increased dramatically (Fig. 4a, inset) while p14 labelling was lost (Fig. 4b, inset).

The data in Table 1 show the corresponding numerical values for the p39 labelling. When viral particles were treated with NP-40 alone, there was very little increase in labelling. However, treatment with DTT alone caused a significant increase in the number of gold particles per virion. This is in agreement with other data, obtained by a novel cryo-EM immunolabelling procedure, which showed that DTT alone is sufficient to cause a dramatic loosening of the membranes surrounding the IMV (48). In this process, the core became exposed and was labelled strongly on its outer side with antibodies to p39. In our experiments, a combination of NP-40 and DTT caused an almost 500-fold increase in labelling relative to the untreated control, suggesting that p39 is associated with the external surface of the core structure.

p39 is protected from protease digestion in intact IMV particles. We confirmed the internal location of p39 by carrying out experiments in which intact purified IMVs were treated with different proteases. Virions were incubated with increasing concentrations of proteinase K, from 5 to 300 μg/ml, for 30 min on ice. Under these conditions, even the highest concentrations of proteinase K did not cause any digestion of p39 while two membrane proteins which are exposed on the outside of the IMV, p32 (D8L) and p14 (A27L) (53), were completely digested (Fig. 5a). The major core proteins, such as 4a-4b (A10L and A3L) and p11 (F18R), were protected. Additional proteases (chymotrypsin and thermolysin) failed to

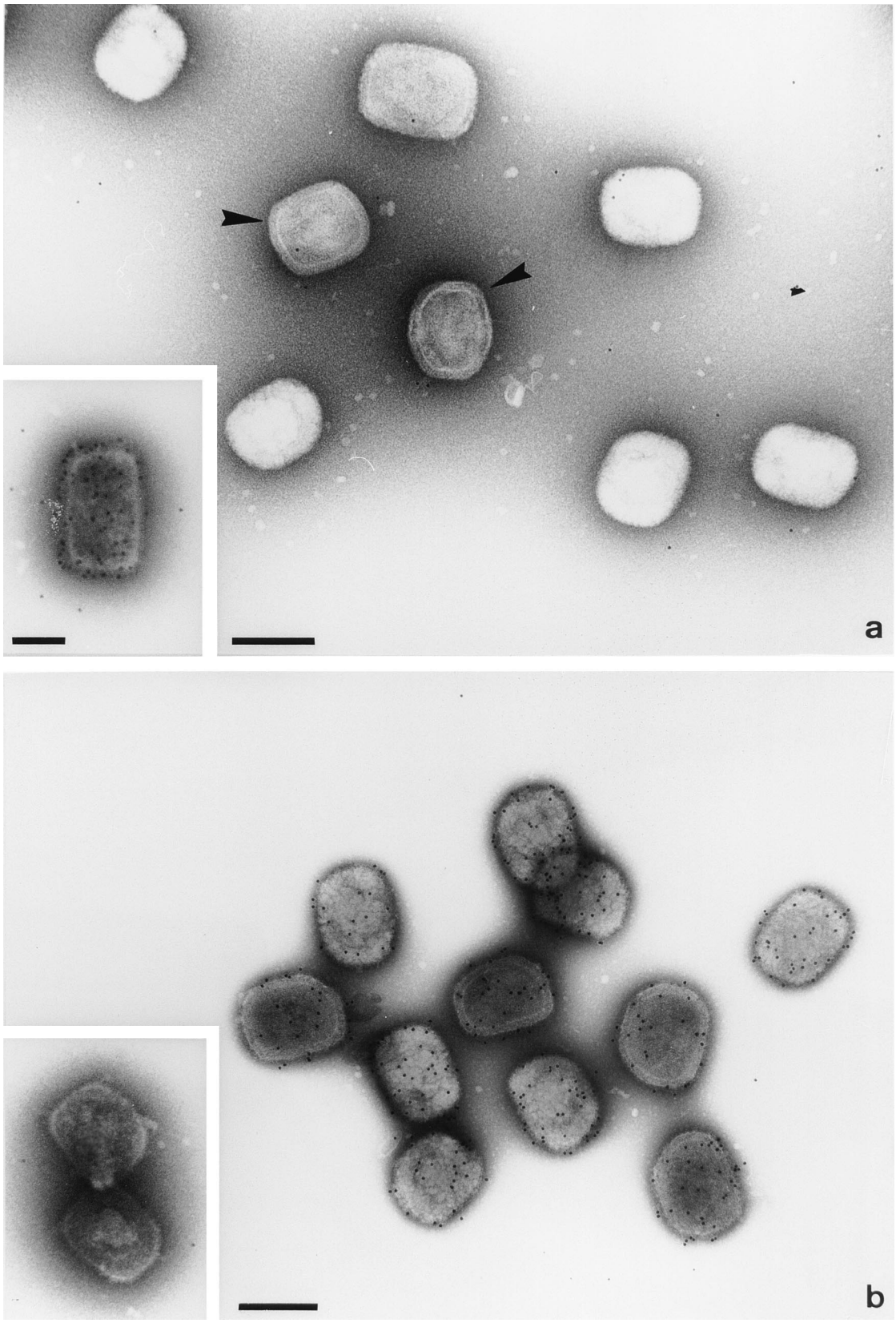

FIG. 4. Immunolabelled and negatively stained IMV as viewed by EM. Purified IMVs were adsorbed to an EM grid and labelled with antibodies against (a) p39 and (b) p14, followed by protein A-gold. The insets show IMV particles which were treated with 1% NP-40 and 20 mM DTT to remove the viral membranes prior to labelling. In contrast to anti-p14, antiserum against p39 does not significantly label intact IMV. However, after NP-40 and DTT treatment, the cores are devoid of p14 labelling while the p39 labelling has dramatically increased. Visible in panel a are virus particles which are open to the negative stain (arrowheads) but do not label with anti-p39, suggesting that the epitope is still masked by the surrounding envelope. Bars, 200 nm (a), 100 nm (a, inset), and 200 nm (b).

TABLE 1. Labeling of intact IMV with α p39 on EM grids[a]

Treatment	No. of gold particles per virion (mean ± SEM)[b]	Ratio[c]
None (control)	0.1 ± 0.01	1.0
NP-40	2.5 ± 0.45	25
DTT	7.5 ± 1.45	75
NP-40 and DTT	47.4 ± 2.08	474
Trypsin	3.1 ± 0.47	31
Proteinase K	0.6 ± 0.02	6

[a] Purified IMV were adsorbed to Formvar- and carbon-coated 100-mesh EM grids and treated as described in Materials and Methods. The grids were subsequently blocked and labelled with anti-p39 antibodies followed by 10-nm protein A-gold.

[b] SEM, standard error of the mean; $n = 20$.

[c] For the ratios, the data for the treated samples were compared with the value for untreated control sample, which was normalized to 1.

digest p39, while they removed p32 and p14 from the outside of the virion (Fig. 5b). V8 had no effect, even on the last two membrane proteins. When longer incubation times of 2 h were used, the core proteins were eventually digested (results not shown), which is in agreement with our previous studies (48). When NP-40- and DTT-isolated cores were treated with protease for 30 min, the particles were completely digested (as ascertained by EM) and there were no polypeptide bands, other than small digestion products, remaining on the gel (data not shown).

p39 associates with viral membranes. Kyte and Doolittle hydrophobicity plots of the p39 sequence show that it does not have any hydrophobic sequence typical of membrane spanning proteins, i.e., a stretch of 17 to 22 hydrophobic amino acids that may adopt an alpha-helical structure, but data in the literature showed that a small amount of p39 was found in the membrane fraction after NP-40 and DTT treatment (35). Therefore, we decided to undertake a detailed biochemical characterization of p39. We used a number of different criteria which are widely used to categorize the physical properties of proteins. First, the membrane proteins of purified IMV were extracted by a classical method for vaccinia virus which involves removal of the viral membranes with a combination of 1% NP-40 and 20 mM DTT, along with some modifications which improved the extraction of membrane proteins, such as p32 (see Materials and Methods). Following this treatment, about 60% of the p39 remained with the core fraction while the remaining 40% was in the membrane fraction (Fig. 6b). As expected, the core proteins 4a, 4b, p25, and p11 (A10L, A3L, L4R, and F18R, respectively) were present exclusively in the core fraction. The extraction of p39 was highly variable, and in some experiments the majority of p39 was found in the membrane fraction. When 2D gels were used for separation, (Fig. 6c), the p39 pattern appeared complex, as the protein was resolved into a number of different spots, the identities of which were confirmed by Western blotting (data not shown). This pattern is very similar to that seen in 2D gels by Oie and Ichihashi (45), who referred to this protein as p37.

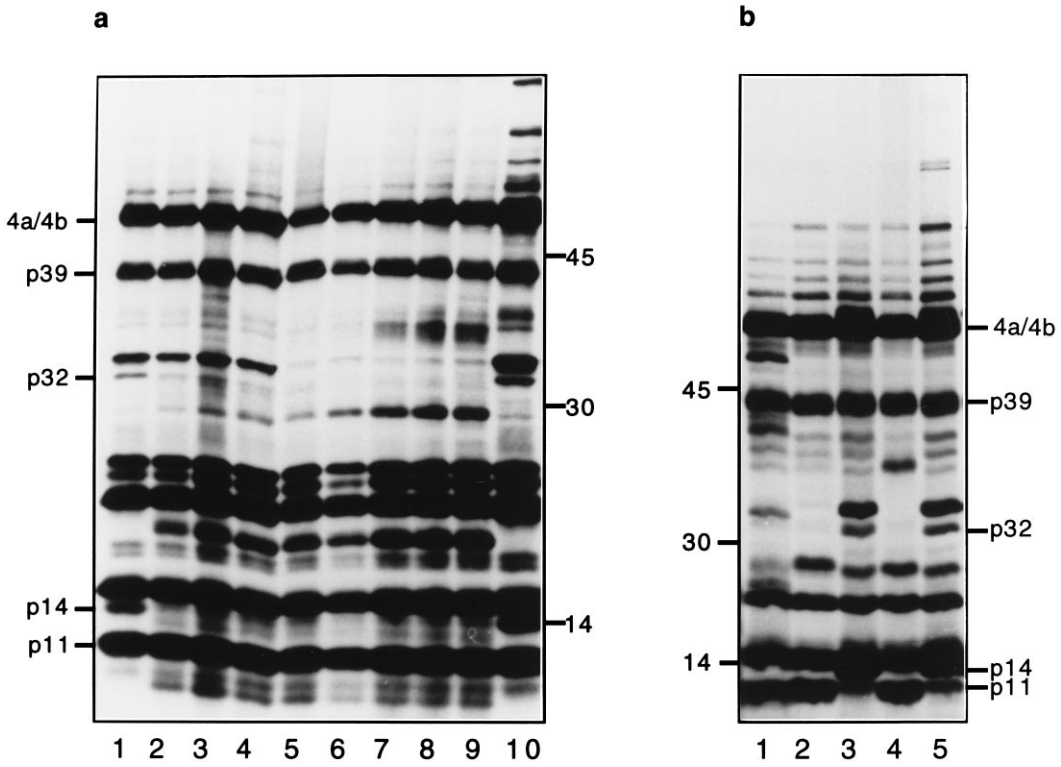

FIG. 5. p39 is not digested during protease treatment of IMV. (a) ^{35}S-labelled purified IMV was treated with proteinase K for 30 min on ice. Lane 1, mock-treated control; lanes 2 to 9, samples treated with 5, 10, 20, 30, 50, 100, 200, and 300 μg/ml proteinase K, respectively; lane 10, untreated IMV sample. The positions of 4a, 4b, p11, and p39, which are not digested, as well as the position of p32, which is sensitive to proteinase K, are indicated on the left. The positions of molecular mass markers (in kilodaltons) are indicated on the right. (b) IMV was also subjected to treatment with 50 μg of α-chymotrypsin per ml (lane 1), 100 μg of thermolysin per ml (lane 2), and 250 μg of V8 per ml (lane 3) at 37°C for 30 min. Lane 4, samples treated with 50 μg of proteinase K per ml for 30 min on ice; lane 5, untreated control IMV. The positions of the major core proteins, 4a, 4b, and p11, as well the membrane protein p14, are indicated on the right, while the positions of three molecular mass markers (45, 30, and 14 kDa) are indicated on the left.

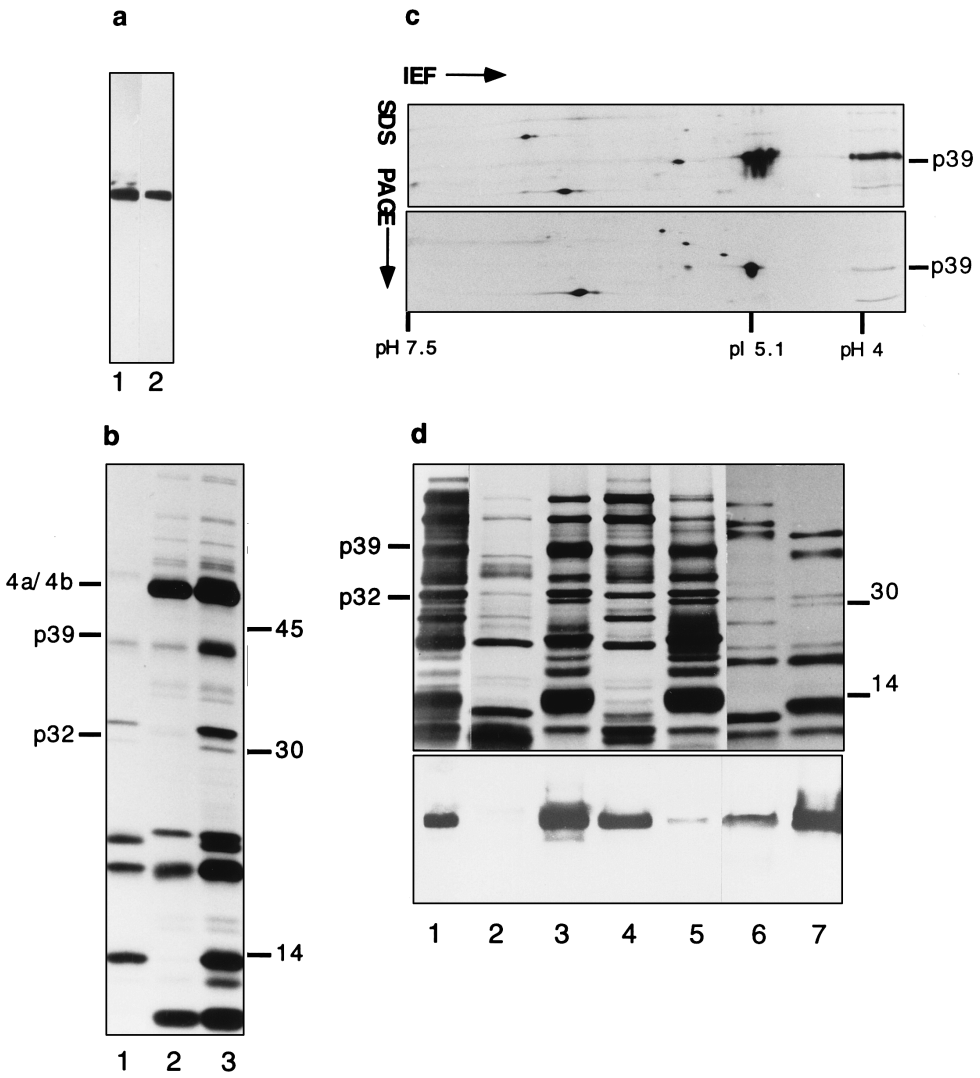

FIG. 6. Membrane association of p39. (a) Immunoblot showing the specificity of the two p39 antibodies used in this study. Lane 1, the C-terminal peptide antiserum; lane 2, antiserum against the entire protein (8). (b) ^{35}S-labelled purified IMV was incubated with 1% NP-40 and 20 mM DTT for 30 min, after which the sample was centrifuged through a 36% (wt/vol) sucrose cushion to pellet the cores. Lane 1, membrane proteins; lane 2, core proteins; lane 3, untreated control IMV. Membrane (p32) and core (4a/4b) proteins are indicated on the left. (c) 2D gel electrophoresis of NP-40- and DTT-treated samples. Isoelectric focusing (IEF) was used in the first dimension, and SDS-PAGE was used in the second dimension. The top panel shows the pelleted core proteins, while the bottom panel shows the membrane protein fraction. Only the relevant part of the autoradiogram is shown. The protein pattern on the right side of the autoradiogram represents the same samples subjected only to SDS-PAGE. The position of p39 is indicated on the right. The pH range of the IEF is shown at the bottom of the gels, and the pI of p39 is also indicated. (d) PNSs from infected cells and purified IMV were subjected to treatment with 1% TX-114 or Na_2CO_3. The top panel shows the gel samples, while the bottom panel shows a Western blot of an equivalent gel probed with anti-p39. Lane 1, untreated control PNS; lane 2, aqueous phase from TX-114-treated PNS; lane 3, detergent phase from TX-114-treated PNS; lane 4, supernatant from Na_2CO_3-treated PNS; lane 5, pellet fraction from Na_2CO_3-treated PNS; lane 6, aqueous phase of TX-114-treated purified IMV; lane 7, detergent phase of TX-114-treated purified IMV. Numbers on the right of panels a and c indicate the positions of molecular mass marker proteins (in kilodaltons).

In another series of experiments, purified IMVs were subjected to treatment with TX-114. Following phase separation, TX-114 separates proteins predominantly according to their hydrophobicity, with hydrophobic and hydrophilic proteins tending to partition into the detergent phase and the aqueous phase, respectively (1). Since membrane proteins contain hydrophobic sequences that anchor them in the membrane, this phase separation technique can be operationally used to separate membrane proteins from soluble proteins. After this extraction technique, p39 was found completely in the detergent phase, indicating that it behaves as a hydrophobic protein (Fig. 6d, lane 7). In order to study the behavior of p39 in the absence of IMV formation, cells were infected in the presence of rifampin to block virus assembly and then radiolabelled from 6 h p.i., and a PNS was subsequently prepared. A comparison of ^{35}S-labelled proteins of such samples with a purified IMV preparation obtained by 2D gel electrophoresis indicated that they were quite similar. Because of the shutoff of host protein synthesis and the labelling times chosen, the PNS contained almost exclusively (late) viral proteins (25). PNSs from these cells were treated with TX-114. Again, p39 was found predominantly in the detergent phase, as was p32 (D8L), which has been previously described as a membrane protein (53) (Fig. 6d, lane 3). These results were unexpected because of the hydrophilic nature of p39 predicted by the Kyte and Doolittle algorithm.

In order to further characterize the membrane association of p39, PNSs from rifampin-blocked infected cells were treated

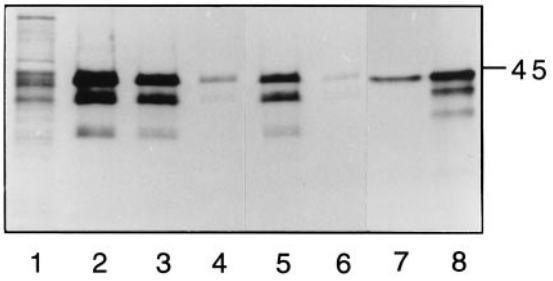

FIG. 7. In vitro translation and translocation of p39. p39 was translated in vitro with a rabbit reticulocyte lysate system. The samples were then immunoprecipitated with antibodies against p39, which yielded three different bands (lane 8), the uppermost of which comigrates with p39 immunoprecipitated from IMV (lane 7). The faster-migrating bands are most likely due to premature termination or internal initiation of the translation. Lanes 1 and 2, aqueous and detergent phases, respectively, of the in vitro translation reaction after TX-14 extraction; lanes 3 to 6, in vitro translation of p39 in the absence (lanes 3 and 4) or presence (lanes 5 and 6) of dog microsomes. After translation, the soluble protein (lanes 3 and 5) was separated from the putative membrane-associated protein (lanes 4 and 6) by centrifugation. The 45-kDa molecular mass standard is indicated on the right.

with Na_2CO_3. This treatment is typically used to establish whether proteins are associated with membranes in a peripheral or an integral manner (16). The sample was adjusted to pH 11 by addition of an equal volume of 0.2 M Na_2CO_3, which removes the peripherally associated and luminal proteins, after which the membranes, along with their integral proteins, were separated from the soluble proteins by centrifugation. In such experiments, approximately 15% of the p39 was associated with the pelleted membrane fraction (Fig. 6d, lane 5) while the remainder was present in the supernatant (Fig. 6d, lane 4). Typical membrane proteins, like p21 (A17L), p32 (D8L), and p16 (A14L), were found exclusively in the pellet fraction, while the soluble core proteins, such as p11 (F18R) and p25 (L4R), remained in the supernatant (Fig. 6d [25]).

When isolated IMVs were subjected to a single round of solubilization with 7 M urea for 60 min at 37°C, approximately 30% of the p39 was extracted, despite the fact that most of the membrane proteins, with the exception of p14 (A27L), a soluble peripheral-membrane protein, and a protein with a molecular mass of approximately 60 kDa, remained in the virion (data not shown).

In vitro translation and translocation studies suggest that p39 is not an integral membrane protein. The biochemical results encouraged us to further investigate the membrane association of p39. In order to ascertain by an independent approach whether p39 is an integral membrane protein or is merely peripherally associated with membranes—for instance, via protein-protein interactions—the gene coding for p39, A4L, was cloned and inserted into the pGEM vector, under the control of the T7 promoter, in order to carry out in vitro translation and membrane translocation experiments. Upon in vitro translation of A4L and immunoprecipitation with antibodies to p39, three bands could be detected, the most prominent of which (Fig. 7, upper bands) comigrated with p39 immunoprecipitated from IMV (Fig. 7, lane 7). The faster-migrating species are possibly due to incomplete translation products. When in vitro-translated p39 was treated with TX-114, most of the protein was found in the detergent phase (Fig. 7, lane 2), showing again that p39 behaves as a hydrophobic protein, even in the absence of other viral proteins. When microsomes were added to the translation system at the beginning of the reaction, p39 failed to insert into these membranes, suggesting that it is not a typical endoplasmic reticulum-synthesized integral membrane protein (Fig. 7, lane 5).

We also investigated whether the membrane association of p39 could be accounted for by fatty acid acylation. However, metabolic labelling with [^{3}H]palmitate or [^{3}H]myristate, followed by immunoprecipitation with anti-p39, indicated that p39 was not modified by the addition of fatty acids (results not shown). However, under our standard immunoprecipitation conditions, we consistently saw a number of other proteins which coimmunoprecipitated with p39, with three of them being especially abundant (Fig. 8, lane 6). One of these proteins was identified as p21 (the product of gene A17L) by immunoprecipitation with antibodies against the C-terminal region of this protein (Fig. 8, lane 7) (31). This is an integral membrane protein which is present in the inner membrane surrounding the IMV (31). The identities of the other bands remain to be established.

Is p39 glycosylated? As early as 1940 it was suggested by Smadel et al. (51) that a vaccinia virus heat-stable basic protein contained small amounts of glucosamine. Moreover, a number of different groups have reported the presence of a glycoprotein with an electrophoretic mobility of 37 to 40 kDa (17, 23, 24, 42, 46). This protein, which can be completely extracted from virions by two rounds of urea extraction (24, 45), has not yet been identified, and therefore we investigated whether p39, which has a similar mobility, could be this glycoprotein. When infected cells were labelled with [^{3}H]glucosamine, the radiolabelled sugar which was reported in the previous studies, a faint band with a very similar molecular weight was found (Fig. 8, lane 1), but unfortunately it was no longer detectable when immunoprecipitated with anti-p39 antibodies (Fig. 8, lane 3). Also, when IMV was subjected to blotting with a monoclonal antibody specific for the O-linked *N*-acetylglucosamine modification (52), a modification that is commonly seen in an ever-increasing list of cytoplasmic proteins (22), a protein with a molecular weight corresponding to that of p39 was detected (data not shown). However, these results were not reproducible, and so we cannot unequivocally conclude that p39 is modified by the addition of O-linked *N*-acetylglucosamine residues. Thus, our results still leave open the possibility that p39 represents the glycoprotein first described by Smadel et al. (51) and further characterized by Holowczak (23), Garon and Moss (17), Moss et al. (42), Ichihashi and Oie (24), and Oie and Ichihashi (46).

As most of the proteins which posess this cytoplasmic O-linked sugar are phosphorylated (22), we also investigated

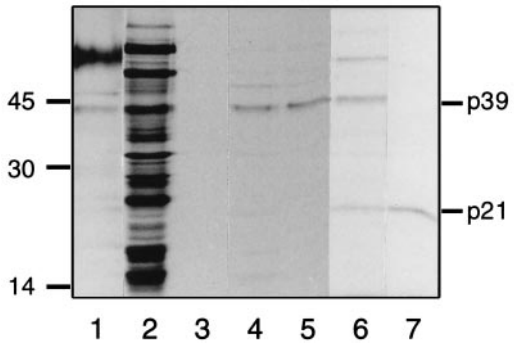

FIG. 8. Immunoprecipitation of p39 from cells infected in the presence of [^{3}H]glucosamine, ^{35}S, or ^{32}P. Lane 1, [^{3}H]glucosamine-labelled PNS; lane 2, ^{35}S-labelled PNS without immunoprecipitation. Immunoprecipitations were performed with antibodies against p39 (8) obtained from [^{3}H]glucosamine-labelled PNS (lane 3), ^{35}S-labelled PNS (lane 4), and ^{35}S-labelled PNS prepared in the presence of tunicamycin, which prevents N glycosylation (lane 5). The immunoprecipitation of p39 (lane 6) shows that p39 may interact with a number of other proteins, one of which was identified as p21 (A17L) by immunoprecipitation with antibodies against the C terminus of this protein (lane 7).

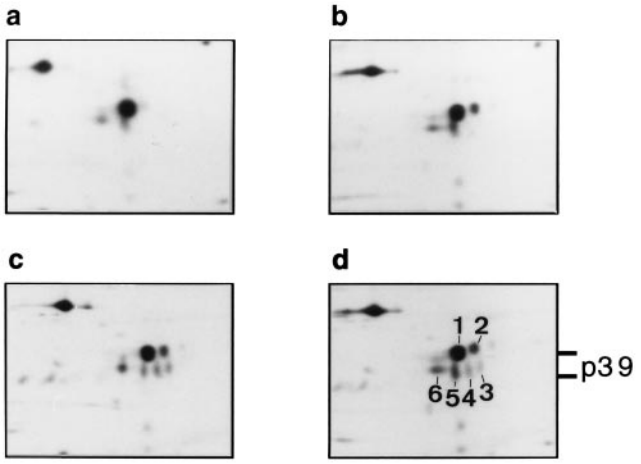

FIG. 9. 2D gel showing pulse-chase analysis of p39. Infected HeLa cells were pulse-labelled for 5 min at 7 h p.i. (a) and chased for 30 min (b), 60 min (c), and 120 min (d). The different forms of p39 that occurred during the various chase times have been numbered 1 to 6 in panel d. Initially, the p39 pattern is quite simple, with a central major spot (no. 1) and some minor species visible (5 and 6). By 60 min of chasing, and even more noticeably by 120 min of chasing, the p39 pattern is more complex, with the central, most abundant form of p39 now surrounded by six other species of varying intensity.

whether p39 was phosphorylated. While a number of viral proteins were labelled by ^{32}P, immunoprecipitation of p39 from the ^{32}P-labelled PNS failed to yield any band, suggesting that p39 is not phosphorylated (results not shown). We also tested for N-linked glycosylation by infecting the cells in the presence of tunicamycin, an N-glycosylation inhibitor, followed by immunoprecipitation with anti-p39. There was no apparent shift in molecular weight of p39 synthesized in the presence of the drug (Fig. 8, lane 5), suggesting that it is not posttranslationally modified by N glycosylation.

Immunoprecipitation experiments in which PNS was probed with antiserum against p39 consistently yielded a number of other proteins (Fig. 8, lane 6). When a complementary sample was immunoprecipitated with an antibody against the C terminus of p21(A17L) (31), a band resulted which comigrated with the lowest of those immunoprecipitated in the experiment with anti-p39 (Fig. 8, compare lanes 6 and 7). This suggests that p39 may associate with p21, which was recently described as an integral membrane protein of the inner membrane of the IMV (31).

Pulse-chase experiments. p39 showed a multiple-polypeptide pattern on a 2D gel, similar to the pattern observed by Oie and Ichihashi (referred to as p37 in reference 45). We next investigated if these different forms were synthesized in a temporal fashion during viral infection by performing pulse-chase labelling experiments followed by separation on 2D gels. In these experiments, the different forms of p39 indeed appeared at different stages during viral maturation. The differently migrating forms have been numbered 1 to 6 in Fig. 9d. The larger central form (form 1) appeared first and was seen after a 5-min pulse, along with a very faint trace of 5 and 6 (Fig. 9a). After a 30-min chase, a fourth form (form 2) appeared (Fig. 9b). Two further species (3 and 4) were apparent after a 60-min chase (Fig. 9c), with little change in the pattern after a 120-min chase (Fig. 9d).

p39 does not form oligomers in vitro. The spike-like structure observed between the membranes and the core in the IMV in all EM studies is approximately 20 nm in length. Therefore, if p39 does form part of this spike, it would most likely need to oligomerize, forming either homo-oligomers or hetero-oligomers with other core proteins. In order to find out if p39 forms homo-oligomers and to obtain a more accurate measure of the apparent molecular weight, in vitro-translated p39 was subjected to high-performance size exclusion chromatography. As can be seen in Fig. 10, p39 behaved as a monomer, eluting from the column with a molecular mass corresponding to 41.5 kDa (± 5%). The peak at 16.3 min, which contains less than 1% of the total protein, corresponds to a molecular mass of 122 kDa (±5%). However, it was confirmed that this peak did not correspond to p39, as their A_{280}/A_{220} ratios were different. Two other, smaller peaks of less than 10 kDa were also eluted. These data indicate that p39 does not form homo-oligomers in vitro. These experiments were very difficult to perform on in vivo-synthesized protein, as p39 cannot be isolated from virions or infected cells without the use of detergent and a reducing agent, both of which could disrupt any potential oligomerization. Therefore, it remains possible that p39 forms homo-oligomers, or even hetero-oligomers, in the virus.

DISCUSSION

The gene product of A4L, a late vaccinia virus gene, has been previously described as a core protein (35). The amino acid sequence of this protein indicates a predicted molecular weight of 30.9 kDa, but on SDS gels it migrates anomalously at a position corresponding to 39 kDa and was therefore referred to as p39 in previous studies (8, 35, 47). It has an unusually high proline content of 30 residues, concentrated mainly in the central region of the protein, which account for 10.6% of the entire protein. From sequence analysis it is evident that there are also a number of internal repeats in p39, which could indicate gene duplication. It has a predominantly hydrophilic nature, as determined by the Kyte and Doolittle algorithm (33), and does not possess a long stretch of hydrophobic amino acids, which protein prediction (PhD prediction program of secondary structure; EMBL) indicates could form a putative membrane-spanning alpha helix. Sequence comparison (Blast program; National Institutes of Health) suggests that p39 has some homology with proteins which have a coiled-coil structure, such as eutrophin and myosins.

Previous studies indicated that p39 was a core protein (33).

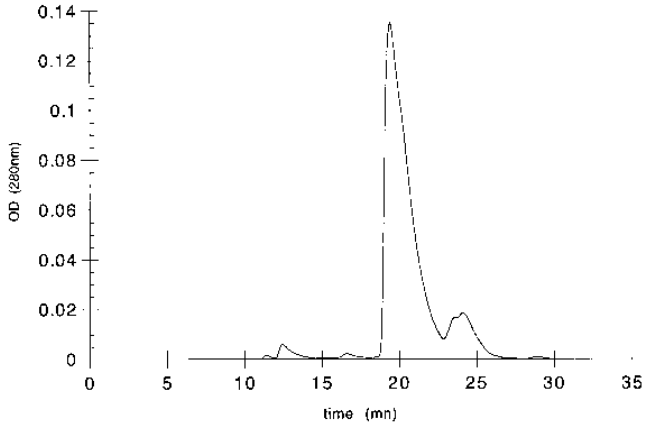

FIG. 10. A graph showing the elution profile of in vitro-translated p39 after high-performance size exclusion chromatography. The *y* axis represents the optical density at 280 nm, while the elution time, in minutes, is shown on the *x* axis. p39 eluted at 19.42 min, which corresponds to 41.5 kDa (±5%) when compared with the calibration standards. Two smaller peaks of 8.9 and 7 kDa are also visible. The peak at 12.5 min is the void volume, while the peak at 16.3 min corresponds to 122 kDa, but analysis of the A_{280}/A_{220} ratio indicated that it is not a trimer of p39.

These results were based on biochemical extraction of IMV with 10 mM DTT and 0.5% TX-100 in 50 mM Tris, pH 8.5, and it was reported that the bulk of p39 was associated with the core. We used a similar technique but adjusted the experimental conditions to obtain the cleanest extraction possible, such that the membrane proteins, e.g., p32 (D8L), p16 (A14L), and p21 (A17L), were found exclusively in the membrane fraction while the core proteins, e.g., 4a-4b (A10L-A3L), were only found in the core fraction. We found that to obtain the most reproducible results, the use of NP-40, as well as DTT at a concentration as high 20 mM, was required. However, we cannot exclude the possibility that such conditions might lead to rearrangements of the core with subsequent extraction of core proteins (e.g., core enzymes) into the membrane fraction. On the basis of our present data (as well as unpublished observations), we suggest the possibility that such core proteins which are lost from the core during NP-40 and DTT treatment may also be located between the membranes and the core of the virion, in a similar manner to p39.

We investigated the localization of p39 throughout the early stages of vaccinia virus assembly by immunogold labelling of cryosections. p39 labels the viral factories very strongly, as well as the central region of the IVs, in a manner which resembles the more typical core proteins, such as 4a (gene A10L) (12, 59), with only a very low amount of membrane association apparent. However, the Na_2CO_3 experiments indicate that a small amount of p39 is associated with membranes in cells which were infected in the presence of rifampin, showing that even before virion assembly has commenced, p39 attains a low degree of membrane association. Upon transition of the IV to the IMV, the pattern of p39 labelling changes dramatically. In the IMV, p39 is located between the two membrane profiles, which are apparent in electron micrographs (Fig. 2b and g and 3c). According to our current interpretation of IMV structure (see the introduction), this would mean that p39 is present in the space between the core and the innermost of the two tightly apposed membranes. In this model, p32 (D8L) is located in the outermost of the two membranes (53) while p21 (A17L) is an integral protein of the inner membrane (31). This interpretation of IMV structure is supported by the fact that when isolated IMVs are treated with DTT alone, the cisternal membranes surrounding the IMV are loosened and begin to come off the virus as one continuous membrane sheath, thereby exposing the underlying core (48). This fact could also explain why p39, a core-associated protein, produces a strong humoral immune response in humans (8, 36); when the virus particles are disrupted in any way, the highly abundant p39 is readily exposed on the outside of the core. Upon DTT treatment of the IMV, spike-like structures which are present between the outer surface of the core and the surrounding membranes of the IMV (5, 10) become exposed, and recent work suggested that p39 might be a component of these spikes (48). All our EM results further support this possibility, as both chemically prepared cores as well as natural cores which arise during vaccinia virus entry into cells (51a) are labelled by anti-p39 on their external surface, where the spikes are exposed.

On our gels, p39 had a molecular mass of 43 kDa, which is even higher than the previously reported value of 39 kDa (8, 35, 47), and when ascertained by gel filtration, the molecular mass of the native protein was 41 kDa. It is difficult to reconcile such a large discrepancy between the predicted molecular mass of 30.9 kDa and the apparent molecular weight mass, even taking into consideration co- or posttranslational modifications. Radiolabelling experiments with ^{32}P, [^{3}H]myristate, and [^{3}H]palmitate indicated that p39 is not modified by either fatty acid acylation or phosphorylation. We also showed that this protein is not modified by the addition of N-linked oligosaccharides. However, there was an indication that p39 may be glycosylated by the addition of *N*-acetylglucosamine, suggesting that it may be the glycoprotein reported by several groups (17, 23, 24, 42, 45), but because of the very low levels of [^{3}H]glucosamine which were incorporated, this point will need further investigation. Therefore, the aberrant migration of p39 on denaturing gels cannot be reconciled by co- or posttranslational modification but may be due in part to the high number of proline residues.

Although our detailed sequence analysis failed to reveal a typical membrane-spanning region, our biochemical data show that p39 has some characteristics typical of a membrane protein. Therefore, we investigated the possibility that p39 may be membrane associated through the addition of a lipid moiety. It has indeed been shown that a number of vaccinia virus proteins can be acylated by the addition of palmitate or myristate (4, 14, 15), although the membrane association of p39 cannot be accounted for by a myristate or palmitate anchor, as the protein cannot be labelled with either [^{3}H]myristate or [^{3}H]palmitate. Moreover, in vitro translation and translocation experiments indicate that the protein does not associate with rough endoplasmic reticulum membranes. Therefore, we postulate that p39 attains its membrane association through interaction with another viral membrane protein(s) in the innermost of the two membranes surrounding the IMV. Coimmunoprecipitation experiments suggest that p21 (A17L) could possibly interact with p39. We have recently identified p21 as an integral protein in the inner membrane of the IMV which spans this membrane four times, with both the N and C termini exposed on the membrane surface which faces the core (31). Thus, the N- and C-terminal regions of p21, as well as the loop region between residues 98 and 118, are ideally located to interact with p39.

Collectively, our data suggest the following model for p39 in the context of vaccinia virus assembly. We propose that p39 is synthesized on free ribosomes in the cytosol and is then transported to the viral factories, as it labels the viroplasm of these factories. Alternatively, the ribosomes may be located within the viral factories. p39 is packaged into the IV, apparently as part of the viroplasm, possibly facilitated by its association with viral membranes even at this early stage (as suggested by the Na_2CO_3 extraction of membranes from cells infected in the presence of rifampin), and subsequently is predominantly located in their central region. However, during transition to the IMV, a new internal core structure develops, and p39 is now located in the space between this newly formed core and the surrounding cisternal envelope, an ideal position in which to act as a matrix protein and to make the link between the core structure and the surrounding membranes. The identity of the spike-like structures, long seen on the surface of the core, must be further investigated in order to establish if p39, possibly along with other proteins, is a structural component of this spike.

ACKNOWLEDGMENTS

We thank R. Jacob for peptide synthesis, R. Kellner for peptide sequencing, L. Gerace for the antibody against the O-linked sugar motif, and B. Dobberstein and K. Schroeder for providing the microsomes as well as technical advice. We also thank A. Sawyer for advice concerning antibody production and G. Vriend for discussions about the sequence of p39.

REFERENCES

1. **Bordier, C.** 1981. Phase separation of integral membrane proteins in Triton X-114 solution. J. Biol. Chem. **256:**1604–1607.
2. **Cairns, J.** 1960. The initiation of vaccinia infection. Virology **11:**603–623.
3. **Cham, B. E., and B. R. Knowles.** 1976. A solvent system for delipidation of

plasma or serum without protein precipitation. J. Lipid Res. **17:**176–181.
4. **Child, S. J., and D. E. Hruby.** 1992. Evidence for multiple species of vaccinia virus-encoded palmitylated proteins. Virology **191:**262–271.
5. **Dales, S.** 1963. The uptake and development of vaccinia virus in strain L cells followed with labeled viral deoxyribonucleic acid. J. Cell Biol. **18:**51–72.
6. **Dales, S., and E. H. Mossbach.** 1968. Vaccinia as a model for membrane biogenesis. Virology **35:**564–583.
7. **Dales, S., and B. G. T. Pogo.** 1981. Biology of poxviruses. Springer-Verlag, Vienna.
8. **Demkowicz, W. E., J. S. Maa, and M. Esteban.** 1992. Identification and characterization of vaccinia virus genes encoding proteins that are highly antigenic in animals and are immunodominant in vaccinated humans. J. Virol. **66:**386–398.
9. **Doms, R. W., R. Blumenthal, and B. Moss.** 1990. Fusion of intra- and extracellular forms of vaccinia virus with the cell membrane. J. Virol. **64:** 4884–4892.
10. **Dubochet, J., M. Adrian, K. Richter, J. Garces, and R. Wittek.** 1994. Structure of intracellular mature vaccinia virus observed by cryoelectron microscopy. J. Virol. **68:**1935–1941.
11. **Easterbrook, K. B.** 1966. Controlled degradation of vaccinia virions *in vitro*: an electron microscopic study. J. Ultrastruct. Res. **14:**484–496.
12. **Ericsson, M., S. Cudmore, S. Shuman, R. C. Condit, G. Griffiths, and J. Krijnse Locker.** 1995. Characterization of *ts*16, a temperature-sensitive mutant of vaccinia virus. J. Virol. **69:**7072–7086.
13. **Essani, K., and S. Dales.** 1979. Biogenesis of vaccinia: evidence for more than 100 polypeptides in the virion. Virology **95:**385–394.
14. **Franke, C. A., P. L. Reynolds, and D. E. Hruby.** 1989. Fatty acid acylation of vaccinia virus proteins. J. Virol. **63:**4285–4291.
15. **Franke, C. A., E. M. Wilson, and D. E. Hruby.** 1990. Use of a cell-free system to identify the vaccinia virus L1R gene product as the major late myristylated virion protein M25. J. Virol. **64:**5988–5996.
16. **Fujiki, Y., A. Hubbard, L., S. Fowler, and P. B. Lazarov.** 1982. Isolation of intracellular membranes by means of sodium carbonate treatment. Application to endoplasmic reticulum. J. Cell Biol. **93:**97–102.
17. **Garon, C. F., and B. Moss.** 1971. Glycoprotein synthesis in cells infected with vaccinia virus. II. A glycoprotein component of the virion. Virology **46:**223–246.
18. **Goebel, S. J., G. P. Johnson, M. E. Perkus, S. W. Davis, J. P. Winslow, and E. Paoletti.** 1990. The complete DNA sequence of vaccinia virus. Virology **179:**247–266.
19. **Griffiths, G.** 1993. Fine structure immunocytochemistry. Springer-Verlag, Heidelberg, Germany.
20. **Grimley, P. M., E. N. Rosenblum, S. J. Mims, and B. Moss.** 1970. Interruption by rifampin of an early stage in vaccinia virus morphogenesis: accumulation of membranes which are precursors of virus envelopes. J. Virol. **6:**519–533.
21. **Harford, C. G., A. Hamlin, and E. Riders.** 1966. Electron microscopic autoradiography of DNA synthesis in cells infected with vaccinia virus. Exp. Cell Res. **42:**50–57.
22. **Hart, G. W.** 1992. Glycosylation. Curr. Opin. Cell Biol. **4:**1017–1023.
23. **Holowczak, J. A.** 1970. Glycopeptides of vaccinia virus. I. Preliminary characterization and hexosamine content. Virology **42:**87–99.
24. **Ichihashi, Y., and M. Oie.** 1980. Adsorption and penetration of the trypsinized vaccinia virion. Virology **101:**50–60.
25. **Jensen, O. N., T. Houthave, A. Shevchenko, S. Cudmore, M. Mann, G. Griffiths, and J. Krijnse Locker.** Identification of the major membrane and core proteins of vaccinia virus by two-dimensional electrophoresis. J. Virol., in press.
26. **Johnson, G. P., S. J. Goebel, and E. Paoletti.** 1993. An update on the vaccinia virus sequence. Virology **196:**381–401.
27. **Joklik, W. K., and Y. Becker.** 1964. The replication and coating of vaccinia DNA. J. Mol. Biol. **10:**452–474.
28. **Katz, E., and B. Moss.** 1970. Formation of a vaccinia virus structural polypeptide from a high molecular weight precursor: inhibition by rifampicin. Proc. Natl. Acad. Sci. USA **66:**677–684.
29. **Katz, E., and B. Moss.** 1970. Vaccinia virus structural polypeptide derived from a high-molecular-weight precursor: formation and integration into virus particles. J. Virol. **6:**717–726.
30. **Krijnse-Locker, J., J. K. Rose, M. C. Hornizek, and P. J. M. Rottier.** 1992. Membrane assembly of the triple-spanning coronavirus M protein—individual transmembrane domains show preferred orientation. J. Biol. Chem. **267:**21911–21918.
31. **Krijnse-Locker, J., S. Schleich, D. Rodriguez, B. Goud, G. Vriend, E. Snijder, and G. Griffiths.** 1996. The role of a 21 kDa viral membrane protein in the assembly of vaccinia virus from the intermediate compartment. J. Biol. Chem. **271:**14950–14958.
32. **Kurzchalia, T. V., J. P. Gorvel, P. Dupree, R. Parton, R. Kellner, T. Houthaeve, J. Gruenberg, and K. Simons.** 1992. Interaction of rab 5 with cytosolic proteins. J. Biol. Chem. **267:**18419–18423.
33. **Kyte, J., and F. Doolittle.** 1982. A simple method for displaying the hydropathic character of a protein. J. Mol. Biol. **157:**105–132.
34. **Laemmli, U. K.** 1970. Cleavage of structural proteins during the assembly of the head of bacteriophage T4. Nature (London) **227:**680–685.
35. **Maa, J.-S., and M. Esteban.** 1987. Structural and functional studies of a 39,000-M_r immunodominant protein of vaccinia virus. J. Virol. **61:**3910–3919.
36. **Maa, J. S., J. F. Rodriguez, and M. Esteban.** 1990. Structural and functional characterization of a cell surface binding protein of vaccinia virus. J. Biol. Chem. **265:**1569–1577.
37. **Morgan, C.** 1976. The insertion of DNA into vaccinia virus. Science **193:** 591–592.
38. **Moss, B.** 1990. Poxviridae and their replication, p. 2079–2111. *In* B. N. Fields and D. M. Knipe (ed.), Virology, 2nd ed. Raven Press, Ltd., New York.
39. **Moss, B.** 1990. Regulation of vaccinia virus transcription. Annu. Rev. Biochem. **59:**661–688.
40. **Moss, B., E. Katz, and E. N. Rosenblum.** 1969. Vaccinia virus directed RNA and protein synthesis in the presence of rifampicin. Biochem. Biophys. Res. Commun. **36:**858–865.
41. **Moss, B., and E. N. Rosenblum.** 1973. Protein cleavage and poxvirus morphogenesis: tryptic peptide analysis of core precursors accumulated by blocking assembly with rifampicin. J. Mol. Biol. **81:**267–269.
42. **Moss, B., E. N. Rosenblum, and C. F. Garon.** 1973. Glycoprotein synthesis in cells infected with vaccinia virus. III. Purification and biosynthesis of the virion glycoprotein. Virology **55:**143–156.
43. **Moss, B., and N. P. Salzman.** 1968. Sequential protein synthesis following vaccinia virus infection. J. Virol. **2:**1016–1027.
44. **Nagayama, A., B. G. T. Pogo, and S. Dales.** 1970. Biogenesis of vaccinia: separation of early stages from maturation by means of rifampicin. Virology **4:**1039–1051.
45. **Oie, M., and Y. Ichihashi.** 1981. Characterization of vaccinia polypeptides. Virology **113:**263–276.
46. **Oie, M., and Y. Ichihashi.** 1987. Modification of vaccinia virus penetration proteins analyzed by monoclonal antibodies. Virology **157:**449–459.
47. **Paez, E., S. Dallo, and M. Esteban.** 1987. Virus attenuation and identification of structural proteins of vaccinia virus that are selectively modified during virus persistence. J. Virol. **61:**2642–2647.
48. **Roos, N., M. Cyrklaff, S. Cudmore, R. Blasco, J. Krijnse-Locker, and G. Griffiths.** 1996. The use of a novel immunogold cryoelectron microscopic method to investigate the structure of the intracellular and extracellular forms of vaccinia virus. EMBO J. **15:**2343–2355.
49. **Schmelz, M., B. Sodeik, M. Ericsson, E. J. Wolffe, H. Shida, G. Hiller, and G. Griffiths.** 1994. Assembly of vaccinia virus: the second wrapping cisterna is derived from the trans Golgi network. J. Virol. **68:**130–147.
50. **Silver, M., and S. Dales.** 1982. Biogenesis of vaccinia: interrelationship between posttranslational cleavage, virus assembly, and maturation. Virology **117:**341–356.
51. **Smadel, J. E., G. I. Lavin, and R. J. Dubos.** 1940. Some constituents of elementary bodies of vaccinia virus. J. Exp. Med. **71:**373–389.
51a. **Snijder, E., et al.** Manuscript in preparation.
52. **Snow, C. M., A. Senior, and L. Gerace.** 1987. Monoclonal antibodies identify a group of nuclear pore complex glycoproteins. J. Cell Biol. **104:**1143–1156.
53. **Sodeik, B., S. Cudmore, M. Ericsson, M. Esteban, E. G. Niles, and G. Griffiths.** 1995. Assembly of vaccinia virus: incorporation of p14 and p32 into the membrane of the intracellular mature virus. J. Virol. **69:**3560–3574.
54. **Sodeik, B., R. W. Doms, M. Ericsson, G. Hiller, C. E. Machamer, W. van't Hof, G. van Meer, B. Moss, and G. Griffiths.** 1993. Assembly of vaccinia virus: role of the intermediate compartment between the endoplasmic reticulum and the Golgi stacks. J. Cell Biol. **121:**521–541.
55. **Sodeik, B., G. Griffiths, M. Ericsson, B. Moss, and R. W. Doms.** 1994. Assembly of vaccinia virus: effects of rifampin on the intracellular distribution of viral protein p65. J. Virol. **68:**1103–1114.
56. **Stern, W., and S. Dales.** 1976. Biogenesis of vaccinia: isolation and characterization of a surface component that elicits antibody suppressing infectivity and cell-cell fusion. Virology **75:**232–241.
57. **VanSlyke, J., S. S. Whitehead, E. M. Wilson, and D. E. Hruby.** 1991. The multistep proteolytic maturation pathway utilized by vaccinia virus P4a protein: a degenerate conserved cleavage motif within core proteins. Virology **183:**467–478.
58. **VanSlyke, J. K., C. A. Franke, and D. E. Hruby.** 1991. Proteolytic maturation of vaccinia virus core proteins: identification of a conserved motif at the N termini of the 4b and 25K virion proteins. J. Gen. Virol. **72:**411–416.
59. **VanSlyke, J. K., and D. E. Hruby.** 1994. Immunolocalization of vaccinia virus structural proteins during virion formation. Virology **198:**624–635.
60. **Wilton, S., A. R. Mohandas, and S. Dales.** 1995. Organisation of the vaccinia envelope and relationship to the structure of the intracellular mature virions. Virology **214:**503–511.
61. **Yang, W. P., S. Y. Kao, and W. R. Bauer.** 1988. Biosynthesis and posttranslational cleavage of vaccinia virus structural protein VP8. Virology **167:**585–590.